Pergamon

Bioorganic & Medicinal Chemistry Letters 11 (2001) 1817–1821

BIOORGANIC & MEDICINAL CHEMISTRY LETTERS

Evaluation of Amino Acid-Based Linkers in Potent Macrocyclic Inhibitors of Farnesyl-Protein Transferase

Douglas C. Beshore,[a,*] Ian M. Bell,[a] Christopher J. Dinsmore,[a] Carl F. Homnick,[a] J. Christopher Culberson,[d] Ronald G. Robinson,[b] Christine Fernandes,[b] Eileen S. Walsh,[b] Marc T. Abrams,[b] Hema G. Bhimnathwala,[b] Joseph P. Davide,[b] Michelle S. Ellis-Hutchings,[b] Hans A. Huber,[b] Kenneth S. Koblan,[b] Carolyn A. Buser,[b] Nancy E. Kohl,[b] Robert B. Lobell,[b] I-Wu Chen,[c] Debra A. McLoughlin,[c] Timothy V. Olah,[c] Samuel L. Graham,[a] George D. Hartman[a] and Theresa M. Williams[a]

[a]*Department of Medicinal Chemistry, Merck Research Laboratories, West Point, PA 19486, USA*
[b]*Department of Cancer Research, Merck Research Laboratories, West Point, PA 19486, USA*
[c]*Department of Drug Metabolism, Merck Research Laboratories, West Point, PA 19486, USA*
[d]*Department of Molecular Systems, Merck Research Laboratories, West Point, PA 19486, USA*

Received 20 February 2001; accepted 25 April 2001

Abstract—A series of amino acid-based linkers was used to investigate the effects of various substituents upon the potency, pharmacokinetic properties, and conformation of macrocyclic farnesyl-protein transferase inhibitors (FTIs). As a result of the studies described herein, highly potent FTIs with improved pharmacokinetic profiles have been identified.

Farnesyl-protein transferase (FPTase) is a zinc metalloenzyme that catalyzes the *S*-alkylation of a cysteine residue in the C-terminal tetrapeptide Ca_1a_2X sequence of proteins with farnesylpyrophosphate (FPP). This post-translational modification localizes the proteins to the cell membrane, enabling them to participate in signal transduction during cellular proliferation.[1] The Ras protein is a substrate of FPTase and has been implicated in 20–30% of all human tumors. In these tumors, mutant Ras loses its GTPase function, becomes constitutively bound to GTP and, when localized to the cell membrane, transmits growth signals independent of extracellular growth factors.[2] Strategies for controlling such unimpeded oncogenic mutant *ras*-driven tumors have focused on preventing the requisite cellular localization of Ras through the use of FPTase inhibitors (FTIs), which have potential as chemotherapeutic agents.[3] FTIs have been identified that mimic the protein substrate, FPP, or both, including small molecule, nonpeptide, nonthiol inhibitors.[4]

In earlier studies, optimization of 1-aryl-2-piperazinones,[5a] in combination with data obtained from transferred NOE NMR experiments, led to the macrocyclic FTI **1**[5b] ($IC_{50} = 0.1$ nM, Fig. 1). Isomeric **2**[5c] ($IC_{50} = 3.5$ nM) is over 10-fold less potent, which suggests that the conformation of the amide and/or the substitution of the amino acid backbone significantly affects potency. Here we report the use of peptide-based template **3** to explore the effects of substitution upon conformation, potency, and the pharmacokinetic profiles of macrocyclic FTIs.

Scheme 1 depicts the synthesis of compounds **4**–**20**. 8-Amino-2-naphthol **21** was *N*-Boc protected, silylated,

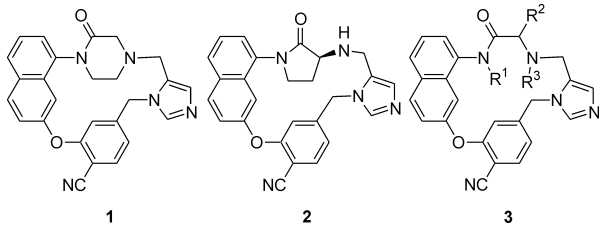

Figure 1. Macrocyclic inhibitors of FPTase.

*Corresponding author. Tel.: +1-215-652-7474; fax: +1-215-652-7310; e-mail: douglas_beshore@merck.com

0960-894X/01/$ - see front matter
PII: S0960-894X(01)00340-7

and deprotected to provide amine **22**. PyBOP-mediated acylation of various amino acids followed by removal of protecting groups afforded amine **24**, which was reductively alkylated with the previously reported aldehyde **26**[5b] to produce the corresponding acyclic phenol. Macrocyclization to give compounds **4**–**16** was accomplished with cesium carbonate in DMF ($\leq$0.01 M to prevent dimerization). For the series in which R^1 = Me, carbamate reduction gave the *N*-methylnaphthalene **23**, which was converted to **25**. Because forcing conditions were required to acylate **23**, partial racemization occurred and enantiopure **25** was obtained via chiral HPLC separation. The amine was reductively alkylated with **26** and cyclized to provide compounds **17**–**20**. The introduction of an alkyl group to the secondary amine at the R^3 position was accomplished by reductive alkylation of the parent macrocycle with formaldehyde or benzaldehyde to give compounds **11**–**16**, **18**, and **20**. Homologated macrocycles were synthesized in analogy with previously reported methods[5c] by an EDC-mediated coupling of the appropriately substituted amine (**24** or **25**) with [1-(4-cyano-3-fluorobenzyl)-1*H*-imidazol-5-yl]acetic acid followed by cyclization to afford compounds **29**–**32**.

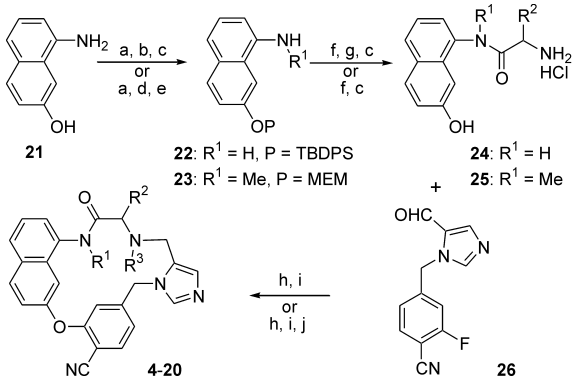

Scheme 1. Reagents and conditions: (a) Boc_2O, THF/DCM, 70 °C, 86%; (b) TBDPSiCl, imidazole, DMF, 60 °C, 96%; (c) HCl (g), EtOAc, 0 °C; (d) NaH, MEMCl, THF, 0 °C–rt, 58%; (e) LAH, THF, 65 °C, 88%; (f) Boc-AA-OH, PyBOP, DIEA, DCM; (g) TBAF, THF; (h) **26**, DIEA, AcOH, $NaCNBH_3$, MeOH; (i) Cs_2CO_3, DMF, 0.01 M, 65 °C; (j) aldehyde, AcOH, $NaCNBH_3$ MeOH.

Scheme 2 depicts the synthesis of compounds **33** and **34**. Compound **21** was converted to 8-iodo-2-naphthol and protected as the TIPS ether. Subsequent transmetalation and carboxylation provided **27**, which was acylated with a mono-Boc protected diamine. Unmasking of the terminal amino group provided **28**, which was converted to macrocycles **33** and **34**. Compound **35** was synthesized from **28** via the aforementioned EDC-mediated coupling, which was subsequently cyclized.

Table 1 shows the effects of modifications to the amino acid template. Compounds were assayed for in vitro activity against FPTase resulting in IC_{50} values for measured inhibition. Variation at R^2 revealed a strong preference for a benzyl substituent (**8**) and moderate tolerance for differences in size and polarity (**4**–**10**). Additionally, the chirality imposed by the addition of an α-R^2 substituent affected potency; the (*R*) enantiomer was preferred over the (*S*) by 2- to 10-fold (cf. **5** vs **6**).[6] Trends associated with substitution at R^3 (**11**–**16**, **18**, and **20**) were dependent upon substitution at R^2. While a large substituent was tolerated at R^3 (**14**), a

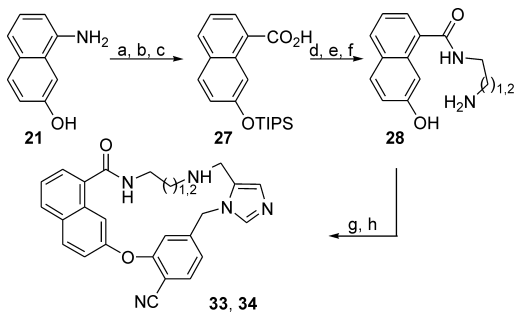

Scheme 2. Reagents and conditions: (a) HCl, $NaNO_2$, KI, THF/H_2O, 93%; (b) TIPSCl, imidazole, DMF, 40 °C, 99%; (c) *t*-BuLi, CO_2, −78 °C; H_2O, TFA, rt, 43%; (d) Boc-diamine, PyBOP, DIEA, DCM; (e) TBAF, THF; (f) HCl, EtOAc, 0 °C; (g) **26**, DIEA, AcOH, $NaCNBH_3$, MeOH; (h) Cs_2CO_3, DMF, 0.01 M, 65 °C.

Table 1. FPTase and GGPTase-I in vitro inhibition and FPTase binding in cell culture for compounds **4**–**20**

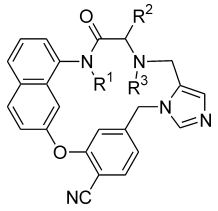

Compd	R^1	R^2	R^3	FPTase in vitro IC_{50} (nM)[a,b]	FPTase binding in cell culture IC_{50} (nM)[c]	GGPTase-I in vitro IC_{50} (μM)[d,b]
4	H	H	H	4.3	37	0.675
5	H	Me (*S*)	H	11	248	4.82
6	H	Me (*R*)	H	1.3[e]	23	0.313
7	H	Et (*R*)	H	1.2	410	0.469
8	H	Bn (*R*)	H	0.47[e]	17	0.066
9	H	2-ThienylCH$_2$ (*R*)	H	2.1	43	0.072
10	H	3-PyridylCH$_2$ (*R*)	H	1.8[e]	1310	0.147
11	H	H	Me	5.7	196	2.07
12	H	Me (*R*)	Me	7.0	>100	1.22
13	H	Bn (*R*)	Me	2.7	184	0.350
14	H	H	Bn	2.6	29.6	>20
15	H	Me (*R*)	Bn	18	240	>20
16	H	Bn (*R*)	Bn	50	574	>20
17	Me	H	H	15	55	6.72
18	Me	H	Me	8.4	13	12.8
19	Me	Me (*R*)	H	16	17	3.16
20	Me	Me (*R*)	Me	14	15	6.76

[a]Concentration of compound required to reduce the human FPTase-catalyzed incorporation of [^{3}H]FPP into recombinant Ras-CVIM by 50% (ref 7a).
[b]All values are n = 2, unless otherwise noted.
[c]Concentration of compound required to displace 50% of a potent, radiolabeled FTI from FPTase in cultured Ha-*ras* transformed RAT1 cells (ref 7b).
[d]Concentration of compound required to reduce the human GGPTase-I-catalyzed incorporation of ^{3}H GGPP (100 nM) into a biotinylated K-Ras-derived peptide [1.6 μM; biotinylated peptide corresponding to the C-terminus of human K-Ras (b-GKKKKKKSKTKCVIM, Research Organics)] by 50%. Assay was run with a 30 min preincubation of enzyme and inhibitor in the presence of 5 mM ATP (ref 7c).
[e]Enzyme concentration 10 pM instead of 1 nM in assay, n = 2.

simultaneous increase in size of R^2 led to diminished inhibitory activity. This suggests that both substituents are trying to access the same hydrophobic pocket in the FPTase active site (cf. **16** and **15** vs **14**). With the addition of a methyl group to the R^1 position (**17**–**20**), a 2- to 10-fold loss of in vitro FPTase inhibitory activity was observed (cf. **19** vs **6**). This is perhaps due to the conformational differences between *N*-H and *N*-Me aryl amides (vide infra).[8]

Table 2 shows homologated macrocycles **29**–**35**. Previous work suggested that to obtain a compound as potent as **1**, ring expansion of the macrocycle may be necessary.[5c] Unfortunately, homologation to a 17-membered ring provided no added potency (cf. **29** vs **4**).

Table 2. FPTase and GGPTase-I in vitro inhibition and FPTase binding in cell culture for 17- and 18-membered macrocycles **29**–**35**

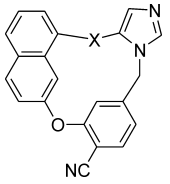

Compd	X	FPTase in vitro IC_{50} (nM)[a,b]	FPTase binding in cell culture IC_{50} (nM)[c]	GGPTase-1 in vitro IC_{50} (μM)[d,b]
29	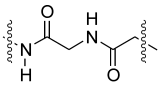	3.8	67	0.150
30	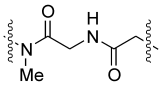	6.6	65	1.09
31	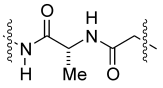	3.3	258	0.050
32	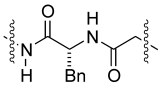	3.5	310	0.029
33	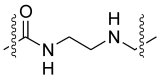	4.5[e]	7.1	0.077
34	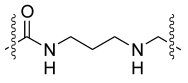	2.3	99	0.89
35	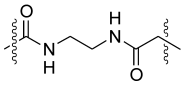	2.5	409	0.250

[a]See footnote a in Table 1.
[b]All values are $n = 2$, unless otherwise noted.
[c]See footnote c in Table 1.
[d]See footnote d in Table 1.
[e]Enzyme concentration 10 pM instead of 1 nM in assay, $n = 2$.

While the 16-membered macrocycles in Table 1 exhibited a preference for a benzyl substituent (**8**), the homologated series was unaffected by amino acid side-chain substitution in the FPTase in vitro assay (cf. **32** and **31** vs **29**). Homologated compounds exhibited a slight loss in potency upon methylation of the *N*-aryl amide (cf. **30** vs **29**). Inversion of the amide connectivity also did not significantly alter potency in vitro (**33**–**35**). Neither additional homologation to an 18-membered macrocycle nor the presence or absence of a carbonyl significantly altered inhibitory activity (cf. **34** and **35** vs **33**).

Activity in cell culture (FPTase binding assay) was measured by an FTI's ability to displace a potent radiolabeled ligand from FPTase.[7b] Compounds **4**–**16** exhibited higher IC_{50} values in cell culture compared to the in vitro assay, perhaps due to poor cellular penetration. Noteworthy was **10**, which contains a side chain with increased polarity that resulted in exceptionally poor activity in cell culture. When the amide *N*-H was replaced with *N*-Me ($R^1 = Me$), cell activity approached or equaled intrinsic potency (**17**–**20**). Homologated macrocycles **30**–**35** also exhibited higher IC_{50} values in cell culture. However, conversion of an amide to an amino group increased activity in cell culture (cf. **30** vs **17** and **35** vs **33**).

Compounds were also assayed for in vitro activity against the related enzyme geranylgeranyl-protein transferase-I (GGPTase-I), which prenylates cellular proteins in a manner analogous to FPTase.[7c] Amide methylation ($R^1 = Me$) increased the GGPTase-I IC_{50} by 4- to 10-fold (cf. **17** vs **4**). Similar to FPTase SAR, substitution at R^2 with small alkyl groups provided no significant change in activity (cf. **6** vs **4**), but the addition of a larger hydrophobic group increased potency nearly 10-fold (cf. **8** vs **4**). The addition of a methyl group at R^3 generally resulted in a 2-fold or greater decrease in inhibitory activity (cf. **18** vs **17**). However, the addition of a benzyl group to R^3 rendered all compounds inactive, regardless of the substitution at R^1 or R^2 (**14**–**16**). Homologated macrocycles **29**–**32** exhibited similar trends; alkylation of the aryl amide resulted in a decrease in potency (cf. **30** vs **29**), and the addition of lipophilicity to the amino acid side chain lowered GGPTase-I IC_{50} values (cf. **32** vs **29**). GGPTase-I potency was generally increased upon homologation to a 17-membered macrocycle (**33** and **29**–**32**) relative to compounds in Table 1 (cf. **30** vs **17**). However, the additional homologation to an 18-membered ring (**34** and **35**) resulted in a decrease in GGPTase-I inhibitory activity (cf. **34** vs **33**).

Pharmacokinetic (PK) data for selected compounds are shown in Table 3.[9] While **1** is a potent FTI, its PK properties are suboptimal. Conversely, **2** is over 10-fold less potent against FPTase and exhibits an increased half-life. Overall, the peptide-based macrocycles described herein have reduced clearances compared to **1**, resulting in increased half-lives. The 3-pyridylmethyl substituted macrocycle **10** was cleared more rapidly, although it had an improved volume of distribution.

In an effort to understand the consistent reduction in FTase inhibitory activity as a result of aryl amide *N*-methylation, we examined the lowest energy conformations of the potent inhibitor **6** and its *N*-Me analogue **19**

Table 3. Pharmacokinetic profiles for selected compounds in dogs[a]

Compd	$T_{1/2}$ (h)	Cl (mL/min/kg)	VD (l/kg)
1	1.0	5.1	0.44
2	3.5	1.1	0.30
4	3.0	2.36	0.55
6	4.8	0.95	0.37
8	2.2	2.23	0.45
9	2.4	1.65	0.26
10	0.8	17.3	0.98
29	3.4	1.49	0.35

[a]Compounds were administered intravenously to two dogs (1 mg/kg) along with 11 other compounds and an internal standard. Plasma extracts were analyzed by LC/MS/MS and reported data is the average of two dogs (see ref 9).

(Fig. 2, top).[10] The most prominent structural difference is the conformation about the amide *N*-C(O) bond. The *N*-H amide in **6** adopts a *cis* amide conformation with respect to the naphthyl and the carbonyl of the amide, while the *N*-Me analogue **19** adopts the opposite amide conformation. These results are consistent with previously reported data regarding the lowest energy conformations of *N*-H and *N*-Me anilides.[8] As a result of these differences, the trajectory of the naphthyl group has changed by nearly 90°. It has been shown in previous studies that the overall orientation of the carbonyl group within the active site of FPTase is an important feature of structurally related, highly potent FTIs.[5d] The lowest calculated energy conformation of **1**[5b] places the carbonyl group in the presumed enzyme-bound conformation.[5d] Best-fit overlays of **6** and **19** onto **1** (Fig. 2, bottom) require that they deviate from their lowest energy conformations by 5.7 and 11.5 kcal/mol, respectively. The higher energy required for the *N*-Me amide to adopt this presumed FPTase-bound conformation relative to **6** may account for its reduced potency. These results reinforce the notion that the orientation of the carbonyl group is important, and imply that the trajectory of the naphthyl group may also play a role in obtaining highly potent FTIs.

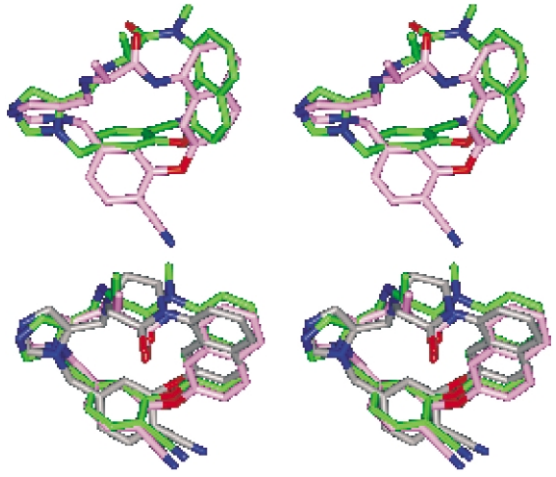

Figure 2. Top: Overlay of calculated lowest energy conformations of **6** (pink) and **19** (green). Bottom: Overlay of **6** (pink, 5.7 kcal/mol relative to lowest energy conformation) and **19** (green, 11.5 kcal/mol relative to lowest energy conformation) with the lowest calculated energy conformation of **1** (see ref 10).

The studies described herein have examined the SAR of amino acid-based linkers of 16-, 17-, and 18-membered macrocyclic FPTase inhibitors. We have identified a series of highly potent compounds that exhibit improved pharmacokinetic profiles relative to **1**. Conformational analysis has provided an enhanced understanding of structural preferences for the binding of macrocyclic inhibitors that contain an amino acid-based linker.

Acknowledgements

The authors thank Dr. A. S. Kim and Dr. B. W. Trotter for manuscript suggestions and Dr. C. S. Hamann for compound analysis of FPTase inhibition.

References and Notes

1. (a) Kato, K.; Cox, A. D.; Hisaka, M. M.; Graham, S. M.; Buss, J. E. *Proc. Natl. Acad. Sci. U.S.A.* **1992**, *89*, 6403. (b) Rowinsky, E. K.; Windle, J. L.; Von Hoff, D. D. *J. Clin. Oncol.* **1999**, *17*, 3631.
2. Rodenhuis, S. *Semin. Cancer Biol.* **1992**, *3*, 241.
3. (a) Gibbs, J. B. *Cell* **1991**, *65*, 1. (b) Gibbs, J. B.; Oliff, A. I. *Annu. Rep. Biopharmacol. Toxicol.* **1997**, *37*, 143.
4. (a) Recent reviews: Williams, T. M. *Expert Opin. Ther. Pat.* **1999**, *9*, 1263. (b) Dinsmore, C. J. *Curr. Opin. Oncol. Endocr. Metab. Invest. Drugs* **2000**, *2*, 26. (c) Bell, I. M. *Expert Opin. Ther. Pat.* **2000**, *10*, 1813.
5. (a) Williams, T. M.; Bergman, J. M.; Brashear, K.; Breslin, M. J.; Dinsmore, C. J.; Hutchinson, J. H.; MacTough, S. C.; Stump, C. A.; Wei, D. D.; Zartman, C. B.; Bogusky, M. J.; Culberson, J. C.; Buser-Doepner, C.; Davide, J.; Greenberg, I. B.; Hamilton, K. A.; Koblan, K. S.; Kohl, N. E.; Liu, D.; Lobell, R. B.; Mosser, S. D.; O'Neill, T. J.; Rands, E.; Schaber, M. D.; Wilson, F.; Senderak, E.; Motzel, S. L.; Gibbs, J. B.; Graham, S. L.; Heimbrook, D. C.; Hartman, G. D.; Oliff, A. I.; Huff, J. R. *J. Med. Chem.* **1999**, *42*, 3779. (b) Dinsmore, C. J.; Bogusky, M. J.; Culberson, J. C.; Bergman, J. M.; Homnick, C. F.; Zartman, C. B.; Mosser, S. D.; Schaber, M. D.; Robinson, R. G.; Koblan, K. S.; Huber, H. E.; Graham, S. L.; Hartman, G. D.; Huff, J. R.; Williams, T. M. *J. Am. Chem. Soc.* **2001**, *123*, 2107. (c) Bell, I. M.; Beese, L. S.; Beshore, D. C.; Bogusky, M. J.; Buser-Doepner, C.; Culberson, J. C.; Gallicchio, S. N.; Gibbs, J. B.; Graham, S. L.; Hartman, G. D.; Heimbrook, D. C.; Huber, H. E.; Kassahun, K.; Koblan, K. S.; Kohl, N. E.; Lobell, R. B.; Rodrigues, D. A.; Taylor, J. S.; Williams, T. M. Enzyme Mechanisms 17th Conference, Marco Island, FL, Jan 3–7, 2001. (d) Dinsmore, C. J.; Bergman, J. M.; Bogusky, M. J.; Culberson, J. C.; Hamilton, K. A.; Graham, S. L. *Org. Lett.* **2001**, *3*, 865.
6. The (*S*) enantiomers of compounds **7**, **8**, **12**, **13**, **15**, **16**, **19**, and **20** fell within this range (data not shown).
7. (a) Graham, S. L.; deSolms, S. J.; Giuliani, E. A.; Kohl, N. E.; Mosser, S. D.; Oliff, A. I.; Pompliano, D. L.; Rands, E.; Breslin, M. J.; Deanna, A. A.; Garsky, V. M.; Scholz, T. H.; Gibbs, J. B.; Smith, R. L. *J. Med. Chem.* **1994**, *37*, 725. (b) Lobell, R.; Gibson, R.; Davide, J.; Kohl, N.; Burns, D. Manuscript in preparation. To assess the potency of the FTIs in cells, we utilized a competitive binding assay to determine the concentration of the FTI required to displace 50% of a radiolabeled FTI from FPTase in cultured v-Ha-*ras* transformed RAT1 cells. This radiotracer, [^{125}I] 4-{[5-({(2*S*)-4-(3-iodophenyl)-2-[2-(methylsulfonyl)ethyl]-5-oxopiperazin-1-yl}-methyl)-1*H*-imidazol-1yl]methyl} benzonitrile, has ~50,000

high affinity binding sites per cell (apparent K_d of $\sim$ 1 nM) in the Rat1 cell line. The nonspecific binding signal, determined by the addition of 1000-fold excess unlabeled competitor FTI, is typically 5-fold lower than the specific binding signal. The assay provides comparable results using a variety of cell lines, and is performed as follows. Cells are seeded at 200,000 cells per well in 24-well tissue culture plates and cultured for 16 h. The radiotracer ($\sim$300–1000 Ci/mmol) is diluted into culture media to a concentration of 1 nM, along with the desired concentration of test FTI, and then added to the cell monolayers. After a 4 h incubation at 37 °C, the cells are briefly rinsed with phosphate-buffered saline, removed from the culture plate by trypsinization, and then subjected to gamma counting using a CobraII® gamma counter (Packard Instrument Company). Dose–inhibition curves and IC_{50} values are derived from a 4-parameter curve-fitting equation using SigmaPlot® Software. (c) Huber, H. E.; Abrams, M.; Anthony, N. J.; Graham, S. L.; Hartman, G. D.; Lobell, R. B.; Lumma, W. L.; Nahas, D.; Robinson, R.; Sisko, J. C.; Heimbrook, D. C. *Proc. Am. Assoc. Cancer Res.* **2000**, *41*, Abstract 2838.

8. Itai, A.; Saito, S.; Toriumi, Y.; Tomioka, N. *J. Org. Chem.* **1995**, *60*, 4715.

9. Olah, T. V.; McLoughlin, D. A.; Gilbert, J. D. *Rapid Commun. Mass Spectrom.* **1997**, *11*, 17.

10. (a) Molecular modeling conformations were generated using metric matrix distance geometry algorithm JG (S. Kearsley, Merck & Co., Inc., unpublished). The generated structures were energy-minimized within Macromodel (ref 10b) using MMFF force field. (b) Mohamadi, F.; Richards, N. G. J.; Guida, W. C.; Liskamp, R.; Caufield, C.; Chang, G.; Hendrickson, T.; Still, W. C. J. *J. Comput. Chem.* **1990**, *11*, 440.